Desalination and Water Treatment
www.deswater.com

doi: 10.5004/dwt.2022.28919

274 (2022) 289–296
October

Decolorization of methyl orange dye by photo-Fenton process using silica gel/iron oxide catalyst

Hassanali Rasouli[a], Momen Khodabakhshi[b], Mohammad Ghorbanpour[c,b,*]

[a]*Material Science and Engineering Department, University of Mohaghegh Ardabili, Ardabil, email: h.rasouli@uma.ac.ir*
[b]*Chemical Engineering Department, University of Mohaghegh Ardabili, Ardabil, email: momen.khodabakhshi12@gmail.com*
[c]*Faculty of Chemical and Petroleum Engineering, University of Tabriz, Tabriz, email: Ghorbanpour@tabrizu.ac.ir*

Received 12 March 2022; Accepted 21 August 2022

ABSTRACT

Dyes are generally considered as serious water pollutants which are massively produced in textile, plastic, leather and dye industries. These contaminants need to be removed from the wastewaters. In this study, we developed a new method for preparing a photocatalyst for degradation of methyl orange dye. For this, a series of silica gel/iron oxide nanocomposites were prepared by a solid phase ion-exchange method. The physical and chemical characteristics of nanocomposites were investigated by scanning electron microscopy, energy-dispersive X-ray spectroscopy (EDX), diffusion reflection spectroscopy (DRS) and adsorption/desorption isotherms of nitrogen Brunauer–Emmett–Teller. Then, there photocatalytic performance was evaluated for the photo-Fenton decolorization of methyl orange dye. The results showed that the synthesized nanocomposite in 3 h had the best color decolorization efficiency of 72.6%. Based on the EDX results, the amount of iron in the synthesized nanocomposites during 1, 3 and 5 h were equal to 1.4, 1.5 and 1.6 wt.%, which were very close to each other. The DRS analysis showed the presence of Fe_xO_y cluster oligomers and large Fe_2O_3 particles in the synthesized nanocomposite. The specific surface area of the silica gel was 340 m^2/g. The ion-exchange reduced the surface area to about 260 m^2/g. The optimal pH in the degradation of dye was about 2, which resulted in 89.4% decolorization. The decolorization efficiency was enhanced with the increase of the amount of photocatalyst in the reaction medium to 10 g/L enhanced; however, further increase had a negative effect on the reaction. Also, the duration of decolorization was increased in the high concentrations of dye. It has been concluded that the solid-state ion-exchange method has a great potential in the production of photocatalysts for methyl orange dye degradation.

Keywords: Solid phase ion-exchange; Silica gel; Iron oxide; Photo-Fenton

1. Introduction

Today, water pollution is among the most devastating issues for the environment. The release of toxic substances into water resources such as lakes, rivers, and oceans and so on, getting dissolved in them, lying suspended in the water or depositing on the bed, so deteriorate the quality of water. Dyes are basically persistent organic pollutants that enter in wastewaters from sources like textile, paint, paper and plastic industries [1]. Such persistent pollutants require proper purifying treatments to remove them from the wastewaters. In this area, advanced oxidation processes such as heterogeneous photocatalysis have emerged as a popular method [2]. These processes are based on the generation of powerful oxidative hydroxyl radicals, which are able to mineralize refractory compounds [3]. Among various advanced oxidation processes, Fenton is a useful and effective one. Fenton oxidation system is based on the reaction of H_2O_2 with Fe(II)/Fe(III) ions [4,5].

* Corresponding author.

Although beneficial for the effectiveness, the usage of iron ions as homogeneous catalysts entails several drawbacks. For example, an effective recycling of the utilized catalyst from the wastewater is of great importance to prevention of extra contamination as well as the reduction in the cost. Also, the expense of appliance and some loss of photocatalyst within the separation stages via centrifugation as well as filtration is the substantial drawbacks [2]. In order to overcome these disadvantages, the photocatalyst could be immobilized over a suitable solid support [6]. In this area, various supports such as activated carbon [7], silica [8–10], clays [11–13] and magnetic compounds [2] have been proposed in literature. Among them, silica gel seems an interesting option due to its low cost, transparency, high surface area, and ion-exchange ability [9,14].

Silica gel and other ion-exchangers constructed from a charged insoluble lattice. Through water purification, the oppositely charged ions are attached to the charged groups of catalyst to provide electrical neutrality. These ions are easily interchangeable. The structure of the silica gel consists of a SiO_4 lattice in which oxygen atoms form Si–O–Si bridges. The remaining oxygen atoms, especially the surface atoms, are free and released to bond with the ions present in the solution outside the gel. Thus, silica gel is composed of structural groups as shown in Fig. 1.

Through last decade, a variety of approaches have been employed for preparing of silica gel/iron oxide composite catalyst like as double-templated synthesis [15], solvent-deficient [16], chemical decontamination [17], co-precipitation [18], and impregnation [19,20]. Most of these methods rely on the use of toxic reducing agents and harmful organic solvents. On the one hand, these chemicals are environmentally hazardous. On the other hand, adding these organic may depress the surface activity of catalyst due to the organic wrapping on the particle surface [21]. The liquid-state ion-exchange can be employed to synthesize metal-ion-exchangeable supports [22]. However, this approach has some drawbacks. Hydration of metal ion in the water may be result in formation of large molecules. It is difficult to exchange these large molecules with the supports. Furthermore, the liquid-state ion-exchange requires a large amount of salt solution, which results in environment pollution. Finally, the amount of exchanged cation is often low [23]. To overcome these drawbacks, recently, solid phase ionic exchange method was developed [24–28]. Compared to the liquid-state ion-exchange, the solid-state ion-exchange is simpler, faster, and more cost-effective. In this method, silica gel is mixed with a metal salt and heated by a furnace at a temperature close to the melting point of the salt. The molten salt penetrates the pores of silica gel and ion-exchange takes place in the molten salt medium.

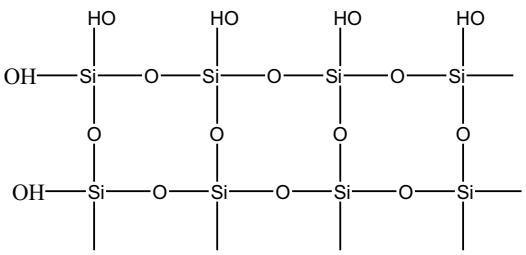

Fig. 1. Silica gel structure.

Recently, solid-state ion-exchanged clays are used for the special purposes like antibacterial agent and catalytic reactions [24–27]. Up to our knowledge, the catalytic properties of silica gel/iron oxide nanocomposites that prepared by solid ion-exchange method are not investigated in photo-Fenton process. So, here, a series of silica gel/iron oxide nanocomposites have been prepared by solid phase ion-exchange method and were used as a photocatalyst for degradation of methyl orange dye by photo-Fenton process. In addition, we attempted to assess the optimal values of process parameters for maximizing of the photocatalyst decolorization efficiency.

2. Experimental

2.1. Chemicals

Silica gel, $FeCl_2$, methyl orange, H_2O_2 (30%) and other reagents were purchased from Merck Company (Germany) and used without further purification.

2.2. Preparation of nanocomposites

Silica gel (10 g) was immersed in molten $FeCl_2{\cdot}4H_2O$ salt (5 g), at 100°C for 1, 3 and 5 h. After ion-exchange, the bentonite was adequately washed with distilled water and sonicated. This step was intended to remove any compounds that were not diffused in the bentonite structure. After filtration, the obtained composites were dried in an oven for 24 h at 25°C.

2.3. Characterization

Scanning electron microscopy (SEM) and energy-dispersive X-ray spectroscopy (EDX) are carried out with an LEO 1430VP Instrument (LEO 1430VP, Germany). A Micromeritics Brunauer–Emmett–Teller (BET) surface area and porosity analyzer (Gemini 2375, Germany) was used to evaluate the products with N_2 adsorption/desorption at the constant temperature of 77 K in the relative pressure range of 0.05–1.00. Absorption spectra of nanocomposites were measured by a UV-Vis Diffusive Reflectance Spectrophotometer (DRS) (Scinco - S4100, Korea) at the wavelength range of 200–700 nm.

2.4. Photo-Fenton activity

The photo-catalytic oxidation experiments were carried out in a 250 mL Pyrex open vessel, placed on a magnetic stirrer and under UVC-lamps (4 W, Philips). The distance between the solution and the UV source was kept constant at 15 cm, in all experiments. After stabilization of the stirring speed ~ 350 rpm, the nanocomposite was introduced into the vessel containing 100 mL of the aqueous solution of MO (250 ppm). Then 8 mM of H_2O_2 was added to the reaction vessel. The moment of adding H_2O_2 was considered as the initial time for reaction. The solution was subsequently stirred for 2 h. During the reaction, liquid aliquots were retrieved from the vessel at selected time intervals. Before

analysis, liquid was centrifuged. Dye removal efficiency was calculated as follows:

$$\text{Discoloration efficiency} = \left[\frac{C_0 - C_t}{C_t}\right] \times 100\% \quad (1)$$

where C_0 and C_t (mg/L) are the liquid-phase concentration of the MB at the initial and any time t respectively, measured by UV-Vis spectrophotometer (Nanolytic, Germany).

3. Results and discussion

3.1. Characterization

The apparent colors of silica gel and solid ion-exchanged silica gel are shown in Fig. 2. According to this figure, the silica gel is purple-gray. After ion-exchange, the color of the nanocomposite changed to yellow and no significant difference was observed in the appearance of the nanocomposites.

The surface morphology of silica gel and solid ion-exchanged silica gel was examined by SEM. As can be seen from Fig. 3, the surface of the silica gel is flat and there are a number of broken pieces of silica gel on its surface (Fig. 3a). The surface of the ion-exchanged nanocomposite prepared in 1 h is similar to silica gel (Fig. 3b). As the ion-exchange time increases, it is observed that more fine particles are formed on the surface (Fig. 3c). These particles have become multiple and larger in number and size during ion-exchange time of 5 h (Fig. 2d). Based on the reactions presented in the introduction section, there are only exchanged iron oxide particles in the nanocomposite prepared in a short time, which cannot show these particles with SEM analysis. By increasing the exchanged ions over time, larger iron oxide particles are formed. These observations are consistent with the results of a study in which a mixture of silica gel and copper sulfate was heated to a temperature close to the melting point of copper sulfate [28]. In the mentioned study, nano leaves were formed on the surface of the glass, which gave antimicrobial properties to the silica gel.

The elemental composition of silica gel surface and solid ion-exchanged silica gel was analyzed using EDX detector and the results are presented in Table 1. According to the obtained values, the formation of nanocomposites through solid-state ion-exchange was confirmed. The parent silica gel did not contain any iron. However, after ion-exchange process there is some iron content in the composition of silica gel. This indicates the success of the ion-exchange process. On the other hand, the amounts of iron in the synthesized nanocomposites during 1, 3 and 5 h were equal to 1.48, 1.55 and 1.66 wt.%, which are very close to each other. Therefore, ion-exchange time did not have a significant effect on the amount of loaded iron and the amount of ion-exchanged iron differed by only 0.2 wt.% during 1 and 5 h. The reason is the mass transfer at a maximum rate of 100°C. At this temperature, iron chloride salt has a molten form; therefore, atomic penetration is done with the highest rate during the first 1 h. This result is consistent with the report of Isalou and Ghorbanpour [11]. In their research, ion-exchange between bentonite and iron chloride was performed in the shortest time at temperature of 100°C, and higher temperatures and process times had no effect on the amount of exchanged iron.

To detect the nature of the iron ion species present in the nanocomposites, the UV-Vis spectra of silica gel and solid ion-exchanged silica gel are shown in Fig. 4. According to the available reports, the adsorption bands of iron ions appear at wavelengths less than 300 nm, the adsorption bands of Fe_xO_y cluster oligomers appear at 300–400 nm, and the adsorption bands at wavelengths higher than 400 nm are related to large Fe_2O_3 particles [27]. The comparison between the spectra for pure silica gel and solid ion-exchanged silica gel indicates that the existing peaks have changed to some extent. According to the obtained spectra, silica gel has a number of peaks in the region of ultraviolet light, that is, the wavelengths less than 314 nm. This region has not changed significantly after the ion-exchange, which indicates the absence of iron ion in the structure of ion-exchanged nanocomposites. This was predictable due to the presence of an oxygen-containing atmosphere during heating in the furnace and the inherent tendency of iron

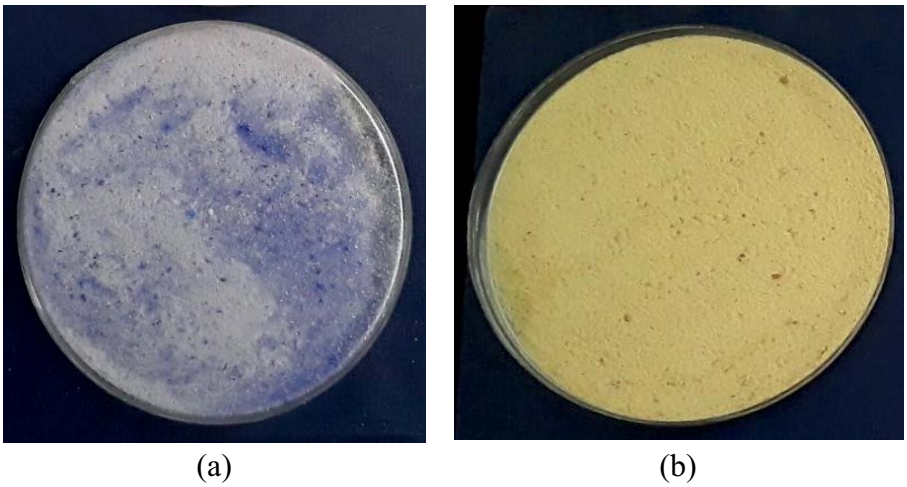

Fig. 2. Appearance of silica gel (a) and solid ion-exchanged silica gel 3 h (b).

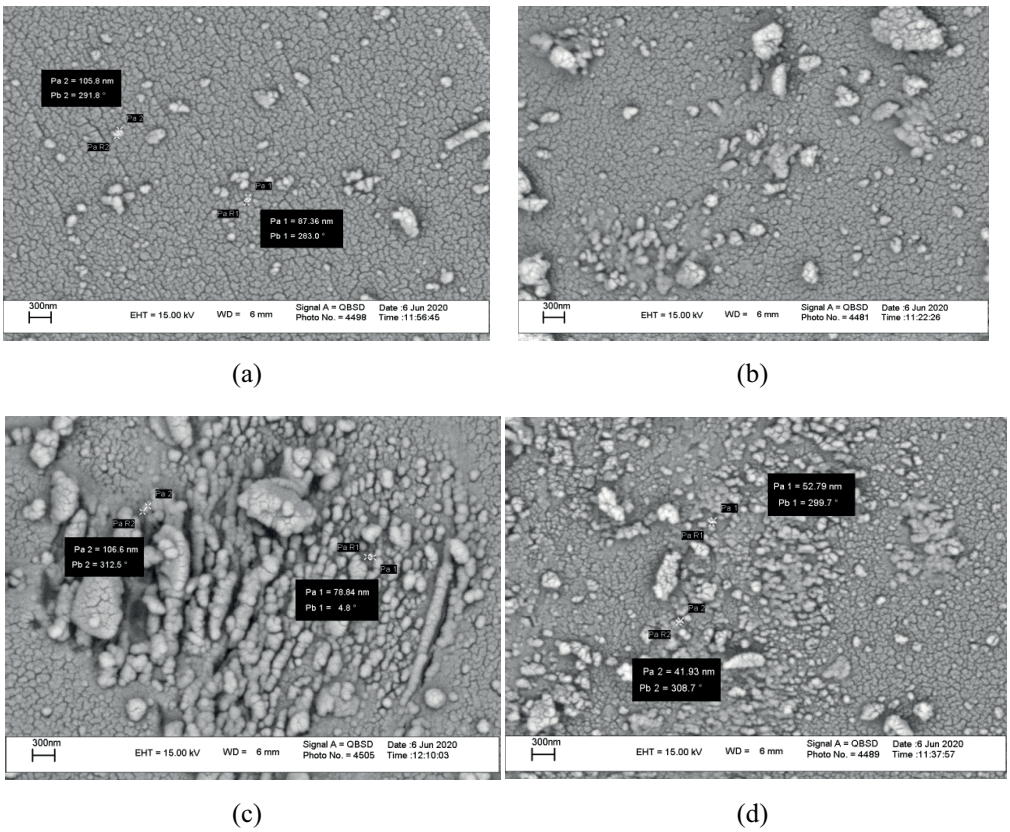

Fig. 3. SEM images of silica gel (a) and solid ion-exchanged silica gel for 1 h (b), 3 h (c) and 5 h (d).

Table 1
Elemental composition (wt.%) of silica gel and solid ion-exchanged silica gel

	Silica gel	Ion-exchange time (h)		
		1	3	5
Oxygen	59.88	57.18	55.67	58.67
Aluminum	0.24	0.31	0.25	0.19
Silicon	39.87	41.017	42.35	39.48
Iron	0	1.48	1.55	1.66

ions to oxidize, so that iron would oxidize rapidly if ionized and did not remain in the ion form. On the other hand, there is a small peak in the wavelength range of 370 nm, and there is a wide peak in the diagram of ion-exchange nanocomposites in the wavelength range greater than 440 nm that were not present in silica gel. This indicates the presence of Fe_xO_y cluster oligomers and large Fe_2O_3 particles in the synthesized nanocomposites.

Table 2 shows the results of the BET analysis. The specific surface area of silica gel is 340 m^2/g. Ion-exchange reduces the surface area by about 260 m^2/g. As this table shows, the pore diameter has not changed through ion-exchange reactions. Since the sizes of the exchanged iron and formed iron oxide particles are very small, no change in pore size is expected. On the other hand, due to the small size of the pores, molten salt will penetrate them very slowly.

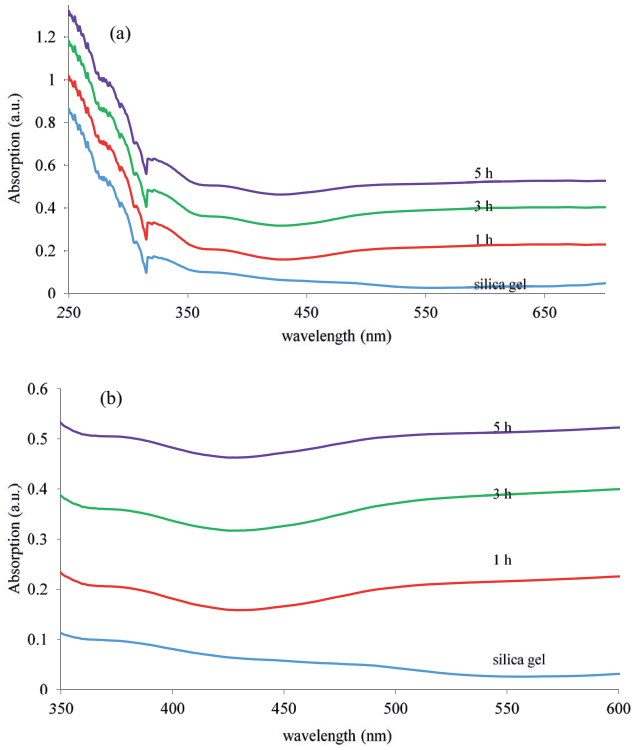

Fig. 4. UV-Vis spectra of silica gel and solid ion-exchanged silica gel in the wider (a) and limited (b) wavelength range.

Therefore, ion-exchange mainly occurs on the surface of the silica gel and the pores are involved in this reaction very slowly. In other words, according to the elemental analysis, the amount of iron in the 1 and 5-h nanocomposites changed insignificantly, which means that the surface experienced relatively complete ion-exchange during the first hour and the following insignificant changes in the amount of iron were due to the ion-exchange in the pores. Accordingly, the pore volume also decreased during the first hour as well. Since the pore diameter has not changed, as shown by electron microscopy images, this is due to the blockage of the pore hole due to the formation of iron oxide particles. As the ion-exchange time increases, the number and size of particles increases while the surface area decreases further.

3.2. Photo-Fenton activity

The results of the decolorization of methyl orange dye by nanocomposites prepared at different times are provided (Fig. 5). The results showed that the rate of degradation of the synthesized nanocomposites at different times is close to each other. The percentages of degradation for the synthesized nanocomposites at 100°C for 1, 3 and 5 h after 15 min were 1.6%, 3.6%, and 5.6%, respectively and they were 70.7%, 72.7% and 71.6% after 2 h. In the first 15 min, there was only a surface adsorption process with little difference between the results. Therefore, the synthesis time has a negligible effect on the adsorption rate of silica gel/iron oxide nanocomposites. Subsequently, the Fenton process was added to the adsorption and at 120 min, the second nanocomposite had a higher efficiency than the other two ones. Therefore, the nanocomposite synthesized at 3 h and 100°C was selected as the optimal nanocomposite.

Based on characterization results, the amount of exchanged iron, specific surface area and morphology in the synthesized nanocomposites were close to each other. The DRS analysis showed the presence of Fe_xO_y cluster oligomers and large Fe_2O_3 particles in the synthesized nanocomposites. Accordingly, it can be concluded that the exchange time has not significant effect on the physicochemical characteristics of the prepared samples and the photocatalytic activities of all samples were close to each other.

The effect of the initial pH of the solution on the methyl orange decolorization is shown in Fig. 6. The pH range between 2 and 4 was studied. The decolorization percentages were 89.4%, 83.8% and 74.0%, at pHs 2, 3 and 4 after 120 min, respectively. It is observed that with increasing pH, the decolorization percentage decreases. Increasing the pH has a destructive effect on the Fenton activity of the catalyst and pH = 2 were considered as the optimal pH. At acidic pH, the rate of degradation of hydrogen peroxide increases because the solubility of ferrous ions is higher and the oxidizing power of hydroxyl radicals is higher [29].

H_2O_2 concentration is an important factor in dye degradation in heterogeneous photo-Fenton processes. Fig. 7 shows the decolorization of methyl orange at different

Table 2
BET analysis of silica gel and solid ion-exchanged silica gel

	Silica gel	Ion-exchange time (h)		
		1	3	5
Pore volume (cm^3/g)	0.2731	0.1896	0.1863	0.1842
Pore diameter (nm)	1.22	1.22	1.22	1.22
Specific surface (m^2/g)	340.01	264.11	262.58	257.36

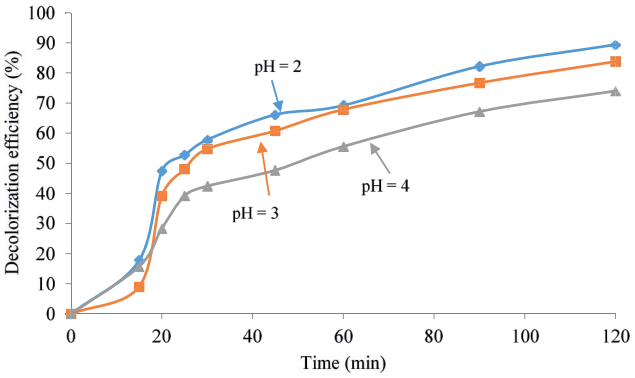

Fig. 6. Effect of pH (initial dye concentration of 250 ppm; 8 mM hydrogen peroxide; 10 g/L of catalyst).

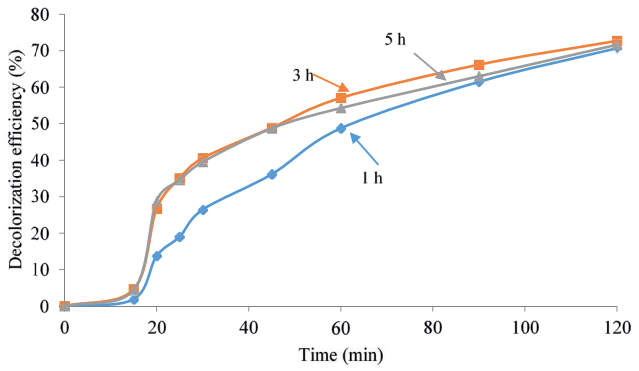

Fig. 5. Decolorization of methyl orange by nanocomposites prepared at different times (initial dye concentration of 250 ppm; 8 mM hydrogen peroxide; 10 g/L of catalyst at pH 3.5).

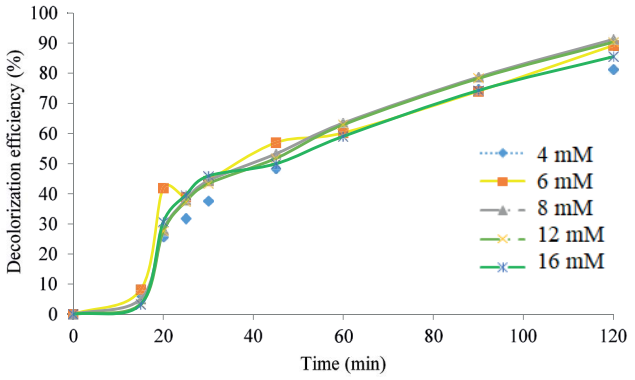

Fig. 7. Effect of hydrogen peroxide concentration on decolorization efficiency (%) (initial dye concentration of 250 ppm; 10 g/L of catalyst at pH 2).

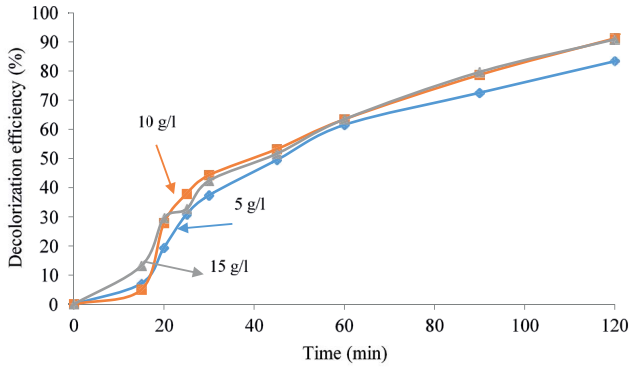

Fig. 8. Effect of catalyst content of aqueous solution on decolorization efficiency (%) (initial dye concentration of 250 ppm; 8 mM H_2O_2 at pH = 2).

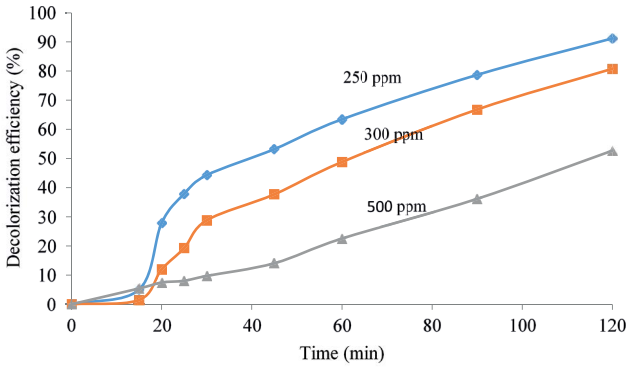

Fig. 9. Investigation of the effect of initial dye concentration (8 mM H_2O_2 at pH 2; 10 g/L catalyst).

concentrations of H_2O_2. As shown in the figure, increasing the concentration of hydrogen peroxide from 4 to 8 mM enhances the dye decolorization efficiency. H_2O_2 is not able to produce hydroxyl radicals at low concentrations; thus, the decolorization efficiency will be low. H_2O_2 decomposes on the surface of the catalyst, and increasing the concentration of hydrogen peroxide leads to the production of more radicals. In the presence of high concentrations of hydrogen peroxide, perhydroxyl radicals are usually produced instead of hydroxyl radicals. Perhydroxyl radicals have a low reactivity and do not participate in oxidative degradation other than organic, which occurs only through reaction with radicals [30]. Therefore, increasing hydrogen peroxide by more than 8 mM reduces the efficiency.

The effect of catalyst content on the decolorization efficiency of methyl orange over time is shown in Fig. 8. The results show that methyl orange decolorization depends on the amount of catalyst and dye decolorization efficiency is enhanced by 5–10 g/L. This is due to the increase in active sites in the presence of higher concentrations of catalyst. On the other hand, by increasing the amount of catalyst to more than the saturation concentration, the penetration of UV light into the solution is prevented. Therefore, increasing the catalyst from 10 to 15 g/L reduced the methyl orange dye decolorization efficiency [31].

Fig. 9 shows the effect of different concentrations of methyl orange dye on dye decolorization efficiency at different time intervals. By increasing the dye concentration from 250 to 500 reduces the dye decolorization efficiency from 91.2% to 48.3%. It is obvious that by increasing the initial dye concentration in the presence of a constant concentration of hydroxyl radicals (due to no change in the catalyst content and the concentration of hydrogen peroxide), the dye decolorization efficiency decreases. Of course, it is necessary to consider light penetration at higher concentrations, which reduces the photocatalytic reaction. Zheng et al. [32] resulted that by increasing the dye concentration from 10 to 100 mg/L, the dye decolorization percentage was drastically reduced, and the dye was completely reduced to 10 mg/L in 90 min.

Fig. 10 indicates that slight dye decolorization was obtained by UV after 2 h, which denotes poor methyl

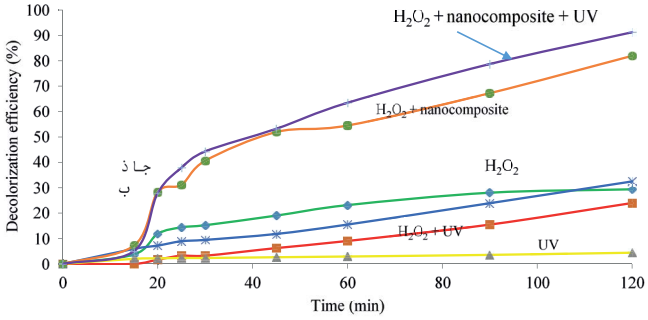

Fig. 10. Optimal nanocomposite catalytic activity according to different methods (8 mM H_2O_2 at pH 2; 10 g/L catalyst).

orange dye degradation by photolysis in the presence of only ultraviolet light. If the adsorbent was used alone, the adsorption rate would be about 29.4%. When the solution was exposed to ultraviolet light plus hydrogen peroxide, the decolorization percentage was 32.5%. After 2 h and in the presence of H_2O_2 and the synthesized catalyst, 81.9% dye decolorization was observed. The best dye decolorization efficiency was observed when the reaction was performed in the adsorbent system + hydrogen peroxide + ultraviolet; so that the degradation rate reached 91.2% after 2 h. The results showed that the color decolorization rate could be improved by ultraviolet light.

For the sake of comparison, Table 3 shows the results of removal of color pollutants with some other synthesized iron/silica nanocomposites. It can be seen that the optimal pH reported for the highest dye decolorization efficiency is about 3. In our study, the decolorization efficiency of 92% was obtained at the reaction time of 2 h when the catalysts amount and the H_2O_2 concentration were 10 g/L and 8 mM, respectively. As it has been mentioned in Fig. 6, the decolorization efficiency in the pH = 2 is slightly higher than pH = 3, so the pH = 2 were considered as the optimal acidity of process. By considering the amount of dye concentration in aqueous solution (250 ppm), it can be said that the performance of the synthesized silica gel/iron oxide catalyst is comparable with the best results reported in literature, while the production method was low-cost, fast and relatively simple to perform.

Table 3
Comparison of the efficiency of iron/silica composites in heterogeneous Fenton removal of pollutant with best results of some previous works

Catalyst	Synthesis method	Pollutant	Reaction condition	Removal	References
Silica gel/iron oxide catalyst	Solid-state ion-exchange	Methyl orange	MO: 250 mg/L; 8 mM H_2O_2; pH = 2; 10 g/L catalyst	91%	This work
Fe (10%)/SBA-15	Impregnation	Methyl orange	MO: 20 mg/L; H_2O_2: 10 mM; pH = 3; UV: 35.8 W/m^2; iron content: 10 wt.%	100% in 90 min 89% of COD in 240 min	[20]
Fe_2O_3-SiO_2 photonic crystal	Double-templated synthesis	Methyl orange	MO: 20 mg/L; catal: 100 mg; H_2O_2: 0.4 mM; pH = 3.0; iron content: 7.6 wt.%	97% in 30 min	[15]
SiO_2/Fe_3O_4	Solvothermal	Rhodamine B	PNP: 10−4 M; iron: 10−4 M; H_2O_2: 10−3 M; iron content: 2.5 wt.%	99% in 24 h	[30]

4. Conclusion

In this study, the silica gel/iron oxide catalysts were successfully prepared using a fast and effective solid-state ion-exchange method. Based on the decolorization efficiency results, the optimal temperature and reaction time for the synthesis of silica gel/iron oxide nanocomposites were 100°C and 3 h, respectively. According to microscopic observations, as the exchange time increased, more iron was ionized with silica gel, which resulted in the formation of more particles on the surface. The EDX analysis showed that the amounts of iron in the synthesized nanocomposites during 1, 3 and 5 h were equal to 1.4, 1.5 and 1.6 wt.%. Also, the DRS analysis indicated the presence of Fe_xO_y cluster oligomers and large Fe_2O_3 particles in the synthesized nanocomposites. The initial specific surface area of silica gel was about 340 m^2/g, while it decreased by 23% after the exchange reaction. Finally, photocatalytic measurements demonstrated that the increasing of the amount of catalyst in the reaction medium enhances the speed and efficiency of the decolorization reaction.

The proposed preparation method for these silica gel/iron oxide catalysts presents new opportunities for producing similar catalysts for photo-Fenton degradation reactions.

References

[1] M. Hassanpour, H. Safardoust-Hojaghan, M. Salavati-Niasari, Degradation of methylene blue and Rhodamine B as water pollutants via green synthesized Co_3O_4/ZnO nanocomposite, J. Mol. Liq., 229 (2017) 293–299.

[2] S. Zinatloo-Ajabshir, M. Salavati-Niasari, Preparation of magnetically retrievable $CoFe_2O_4$@SiO_2@$Dy_2Ce_2O_7$ nanocomposites as novel photocatalyst for highly efficient degradation of organic contaminants, Composites, Part B, 174 (2019) 106930, doi: 10.1016/j.compositesb.2019.106930.

[3] M. Salimi, A. Esrafili, M. Gholami, A.J. Jafari, R.R. Kalantary, M. Farzadkia, M. Kermani, H.R. Sobhi, Contaminants of emerging concern: a review of new approach in AOP technologies, Environ. Monit. Assess., 189 (2017) 414, doi: 10.1007/s10661-017-6097-x.

[4] F. Martínez, G. Calleja, J.A. Melero, R. Molina, Iron species incorporated over different silica supports for the heterogeneous photo-Fenton oxidation of phenol, Appl. Catal., B, 70 (2007) 452–460.

[5] S. Li, Q. Wang, H. Yu, T. Ben, H. Xu, J. Zhang, Q. Du, Preparation of effective Ag-loaded zeolite antibacterial materials by solid phase ionic exchange method, J. Porous Mater., 25 (2018) 1797–1804.

[6] A. Babuponnusami, K. Muthukumar, A review on Fenton and improvements to the Fenton process for wastewater treatment, J. Environ. Chem. Eng., 2 (2014) 557–572.

[7] M. Ghorbanpour, B. Hakimi, A. Feizi, A comparative study of photocatalytic activity of ZnO/activated carbon nanocomposites prepared by solid-state and conventional precipitation methods, J. Nanostruct., 8 (2018) 259–265.

[8] J.V. Coelho, M.S. Guedes, R.G. Prado, J. Tronto, J.D. Ardisson, M.C. Pereira, L.C.A. Oliveira, Effect of iron precursor on the Fenton-like activity of Fe_2O_3/mesoporous silica catalysts prepared under mild conditions, Appl. Catal., B, 144 (2014) 792–799.

[9] T.V. Kon'kova, A.M. Katalevich, P.A. Gurikov, A.P. Rysev, N.V. Men'shutina, Heterogeneous Fenton catalysts based on mesoporous silica gels prepared by drying in supercritical carbon dioxide, Russ. J. Phys. Chem. B, 8 (2014) 999–1003.

[10] S. Zinatloo-Ajabshir, S. Mortazavi-Derazkola, M. Salavati-Niasari, Nd_2O_3-SiO_2 nanocomposites: a simple sonochemical preparation, characterization and photocatalytic activity, Ultrason. Sonochem., 42 (2018) 171–182.

[11] S.K. Isalou, M. Ghorbanpour, Catalytic activity of Fe-modified bentonite in heterogeneous photo-Fenton process, Desal. Water Treat., 162 (2019) 376–382.

[12] B. Hakimi, M. Ghorbanpour, A. Feizi, ZnO/bentonite nanocomposites prepared with solid-state ion-exchange as photocatalysts, J. Ultrafine Grained Nanostruct. Mater., 51 (2018) 139–146.

[13] M. Ghorbanpour, S. Lotfiman, A. Nouri, Diffusion of Cu ions into nanoclay by molten salt ion-exchange for antibacterial application, J. Phys. Sci., 29 (2018) 31–42.

[14] P.S. Shinde, P.S. Suryawanshi, K.K. Patil, V.M. Belekar, S.A. Sankpal, S.D. Delekar, S.A. Jadhav, A brief overview of recent progress in porous silica as catalyst supports, J. Compos. Sci., 5 (2021) 75, doi: 10.3390/jcs5030075.

[15] A. Abdipoor, A. Taheri, A. Rangin, New magnetic graphene oxide core–shell functionalized SBA-15 dual template imprinted polymer for μ-solid phase extraction of nortriptyline and amitriptyline in mice plasma, Sep. Purif. Technol., 298 (2022) 121615, doi: 10.1016/j.seppur.2022.121615.

[16] M.A. Adnan, O. Muraza, S.A. Razzak, M.M. Hossain, H.I. de Lasa, Iron oxide over silica-doped alumina catalyst for catalytic steam reforming of toluene as a surrogate tar biomass species, Energy Fuels, 31 (2017) 7471–7481.

[17] D. Gómez-Carnota, J.L. Barriada, R. Herrero, Green iron doped silica gel materials for one-step chemical decontamination, SSRN Electron. J., (2022) 1–38, doi: 10.2139/ssrn.4097394.

[18] A.V. Tyumentseva, R.N. Yaroslavtsev, S.V. Stolyar, A.T. Saitova, E.S. Tyutrina, A.S. Gorbenko, M.A. Stolyar, I.A. Olkhovskiy, Silica-coated iron oxide nanoparticles for DNA isolation for molecular genetic studies in hematology, Genet. Test. Mol. Biomarkers, 25 (2021) 611–614.
[19] R. Jinisha, R. Gandhimathi, S.T. Ramesh, P.V. Nidheesh, S. Velmathi, Removal of rhodamine B dye from aqueous solution by electro-Fenton process using iron-doped mesoporous silica as a heterogeneous catalyst, Chemosphere, 200 (2018) 446–454.
[20] M.D. Alcalá, C. Real, Synthesis based on the wet impregnation method and characterization of iron and iron oxide-silica nanocomposites, Solid State Ionics, 177 (2006) 955–960.
[21] M. Ghorbanpour, S. Lotfiman, Solid-state immobilisation of titanium dioxide nanoparticles onto nanoclay, Micro Nano Lett., 11 (2016) 684–687.
[22] B. Hakimi, M. Ghorbanpour, A. Feizi, A comparative study between photocatalytic activity of ZnO/bentonite composites prepared by precipitation, liquid-state ion-exchange and solid-state ion-exchange methods, J. Water Environ. Nanotechnol., 3 (2018) 273–278.
[23] N. Farhadian, S. Liu, A. Asadi, M. Shahlaei, S. Moradi, Enhanced heterogeneous Fenton oxidation of organic pollutant via Fe-containing mesoporous silica composites: a review, J. Mol. Liq., 321 (2021) 114896, doi: 10.1016/j.molliq.2020.114896.
[24] B. Hakimi, M. Ghorbanpour, A. Feizi, ZnO/bentonite nanocomposites prepared with solid-state ion-exchange as photocatalysts, J. Ultrafine Grained Nanostruct. Mater., 51 (2018) 139–146.
[25] M. Ghorbanpour, Soybean oil bleaching by adsorption onto bentonite/iron oxide nanocomposites, J. Phys. Sci., 29 (2018) 113–119.
[26] M. Ghorbanpour, M. Mazloumi, A. Nouri, S. Lotfiman, Silver-doped nanoclay with antibacterial activity, J. Ultrafine Grained Nanostruct. Mater., 50 (2017) 124–131.
[27] R. Shayegh, M. Ghorbanpour, A new approach for the preparation of iron oxide-pillared bentonite as adsorbent of dye, Desal. Water Treat., 183 (2020) 404–412.
[28] M. Ghorbanpour, M. Moghimi, S. Lotfiman, Silica-supported copper oxide nanoleaf with antimicrobial activity against *Escherichia coli*, J. Water Environ. Nanotechnol., 2 (2017) 112–117.
[29] L. Liu, S. Liu, S.B. Mishra, L. Sheng, An easily applicable and recyclable Fenton -like catalyst produced without wastewater emission and its performance evaluation, J. Cleaner Prod., 234 (2019) 653–659.
[30] M. Faraji, Y. Yamini, M. Rezaee, Magnetic nanoparticles: synthesis, stabilization, functionalization, characterization, and applications, J. Iran. Chem. Soc., 7 (2010) 1–37.
[31] G.-T. Wei, C.-Y. Fan, L.-Y. Zhang, R.-C. Ye, T.-Y. Wei, Z.-F. Tong, Photo-Fenton degradation of methyl orange using $H_3PW_{12}O_{40}$ supported Fe-bentonite catalyst, Catal. Commun., 17 (2012) 184–188.
[32] H. Zheng, Y. Pan, X. Xiang, Oxidation of acidic dye Eosin Y by the solar photo-Fenton processes, J. Hazard. Mater., 141 (2007) 457–464.